

Analysis of fading statistics in cellular mobile communication systems

Zia M. Loni · Noor M. Khan

Published online: 13 June 2012
© Springer Science+Business Media, LLC 2012

Abstract Spatial channel models are often proposed for modeling the angular aspects of mobile radio channel in picocell, microcell, and macrocellular environments. These models are validated through comparison with available measurement results. The comparisons are usually based on the fitness of their pdfs of angle of arrival to the histogram of occurrences of the signals over an angular span, given in the measurement data. This paper presents a comparison of the notable scattering models with various spatial channel measurements. The paper suggests criteria for the comparative analysis of the previously proposed spatial channel models and measurements on the basis of their fading statistics. Quantitative analysis of the considered models and the field measurements is also presented using multipath shape factors i.e. angle spread, the angular constriction and direction of maximum fading. Based on the obtained shape factors, fading statistics like level crossing rates, average fade duration, auto-covariance and coherence distance are evaluated. Effect of increasing Doppler spread on the level crossing rates and average fade duration is also elaborated in detail.

Keywords Geometrical and statistical channel models · Spatial channel measurements · Level crossing rates · Average fade duration · Coherence distance · Autocorrelation · Fading statistics

Z.M. Loni (✉)
COMSATS Institute of Information Technology, Abbottabad, Pakistan
e-mail: zialoni@ciit.net.pk

N.M. Khan
Muhammad Ali Jinnah University, Islamabad, Pakistan

1 Introduction

Increasing wireless data demand has made researchers to use adaptive antenna arrays in MIMO communication systems. To have efficient utilization of theoretical capacity bounds of the wireless communication link, an understanding of the channel's fading statistics is required. Use of directional antennas has changed the channel's fading statistics in such a way that omnidirectional models are no longer applicable. Numerous Statistical and Geometrical models have been proposed like ring model [1], circular scattering model [2], elliptical scattering model [2], eccentro-scattering model [4], Gaussian scattering density model GSDM [5], and Joint Gaussian scattering model JGSM [6], which are applicable to their specific spatial environment. This is because the probability density function (PDF) changes its shape depending upon the shape of the physical scattering region in micro, pico and macrocellular environment. Moreover, in order to avail the actual information of the scattering channel, a number of experiments have been conducted by researchers like Pedersen et al. [7], Spencer et al. [8], Cramer et al. [9], Jalden et al. [10], and Zhang et al. [11], in different spatial environments. Spatial channel models are validated with the data obtained in these measurement campaigns. Comparison between models and measurement is usually based on the matching of PDF of the angle of arrival to the histogram of occurrences of the signal over an angular span [6]. This paper suggests a non-conventional criterion for the comparative analysis of the previously proposed spatial channel models and measurements on the basis of their fading statistics. A comprehensive literature survey is presented for the overview of spatial channel models and prospective measurements.

A number of attempts have been made to measure the angle of arrival distribution of the multipath components. One of the such campaigns was performed by Pedersen et al. [7]. They conducted experiments in an urban environment having four to six storey buildings. They measured power azimuth (PAS) and power azimuth delay spectrum (PADS) for BS antenna. Measurement data of Pedersen et al. [7] were later compared with a number of scattering models i.e. CSM (Circular Scattering Model), ESM (Elliptical Scattering Model), GSDM and Eccentro-scattering model. ESM consisting of an ellipse with BS and MS at its focal points was proposed by Ertel et al. [2], for angle of arrival (AOA) distribution in microcellular environment. Scatterers were assumed to be uniformly distributed through out the ellipse. BS was modeled with low antenna height. Due to low antenna heights, multipaths arriving at BS experienced reflections near BS as well as around MS. On the other hand, CSM was proposed for macrocellular environment where antenna heights are usually higher as compared to microcellular environment. Scatterers were assumed to be uniformly distributed and restricted in a circle around MS. Due to increased antenna heights, BS was supposed to be free of scatterers. In [2], CSM model employed with directional antennas at the base station was used to study Doppler characteristics of the channel. Directional antenna proved to be useful in rejecting multipaths falling out of the beam range of the antenna. In [5], Janaswamy et al. proposed a Gaussian Scattering Density Model (GSDM) assuming Gaussian distribution of scatterers both at BS and MS. In comparison of GSDM, ESM and CSM with the measurement data of Pedersen et al., Janaswamy showed that GSDM gave good results but the tails of the

measurement campaign could not match its theoretical PDF. By changing the standard deviation of the scatterers around the MS, GSDM was supposed to be applicable to micro, macro and picocellular environments. Due to this advantage, GSDM was also compared with the indoor measurements of Spencer et al. [8], taken in an office building. They used a reflector(dish) antenna operating at frequency of 7 GHz. GSDM was claimed to match well with the practical measurement of Spencer et al. [8]. In [6], Khan et al. proposed Eccentro-scattering model and Jointly Gaussian Scattering Models (JGSM). JGSM in comparison to GSDM proposed two separate Gaussian functions one each at BS and MS. Eccentro-scattering model consisted of an ellipse having BS and MS at its focal points. Eccentro-scattering model and JGSM could be used jointly or independently to model any type cellular environment due to flexibility in the choice of eccentricity of the ellipse. PDF obtained through this model exactly matched the practical measurements. Also the tails of the measurement data of Pedersen et al. exactly matched the theoretical PDF. Measurement data obtained by Pedersen et al. [7], and Spencer et al. [8], are mostly used by researchers to fit their spatial models to the practical environments. Nevertheless, a number of measurement campaigns were launched in the last decade to capture the realistic channel characteristics. Some notable measurement campaigns of that era are Jalden et al. for urban environment [10], and Cramer et al. [9] and Zhang et al. [11] for indoor environment. Moreover, Nawaz et al. in [12] proposed a 3-D model for macrocellular environment with directional antenna placed at BS. Their model could be used for the AOA distribution utilizing both elevation and azimuth planes. However, it has not been compared with measurements.

Geometrically based spatial channel models are only helpful in designing cellular structures if they can match the realistic time-varying scattering behavior of the channel, while there exists a relative motion between mobile and base stations. As far as the analysis of the measurement data and its comparison with geometrical models regarding spatial characteristics is concerned, comparatively little work has been done on its second order statistics. This paper suggests a non-conventional approach for the comparative analysis of the previously proposed spatial channel models on the basis of their fading statistics. Multipath shape factors proposed by Durgin et al. in [13, 14] are helpful in characterizing multipath AOA in non-omnidirectional propagation. This paper thus makes use of the second order statistics based on these shape factors and analyzes various spatial AOA distributions and measurements discussed earlier in this section on the basis of the angle spread, the angular constriction, direction of maximum fading, level crossing rate, average fade durations, auto-covariance and coherence distance. We then compare the results with the statistical expressions of theoretical models and try to validate the assumptions made in their derivations.

2 Proposed Methodology and System Model

Our proposed system model for calculating fading statistics is based on the methodology used by Durgin et al. [13] and Khan et al. [6]. They analyzed the PDF of AOA, $p(\theta)$, using either its Fourier coefficients or trigonometric moments. The above two methods yield the same result but we use the latter method because it is beneficial in

manipulating directional data easily. Moreover, this method gives information about the physical dimensions of the shape factors i.e. it relates shape factors to the standard deviation of the angular energy distribution and gives physical information about the dispersion of the angular data.

The n th complex trigonometric moments, \bar{R}_n , of any angular energy distribution, $p(\theta)$, are defined as

$$\bar{R}_n = \bar{C}_n + j\bar{S}_n \tag{1}$$

where

$$\bar{C}_n = \frac{1}{P_0} \int_{i=1}^N p(\theta) \text{Cos}(n\theta) d\theta \tag{2}$$

and

$$\bar{S}_n = \frac{1}{P_0} \int_{i=1}^N p(\theta) \text{Sin}(n\theta) d\theta \tag{3}$$

In case of discrete measured and observed data, the definition for the trigonometric parameters, \bar{C}_n and \bar{S}_n , can be re-written as

$$\bar{C}_n = \frac{1}{F_0} \sum_{i=1}^N f_i \text{Cos}(n\theta_i) \tag{4}$$

and

$$\bar{S}_n = \frac{1}{F_0} \sum_{i=1}^N f_i \text{Sin}(n\theta_i) \tag{5}$$

where $F_0 = \sum_{i=1}^N f_i$ for $i = 1, \dots, N$ and f_i is the number of occurrences for the AOA, (θ_i) , in the i th bin of histogram.

\bar{R}_n can also be written as

$$\bar{R}_n = |\bar{R}_n| e^{j\bar{\theta}_n} \tag{6}$$

where $|\bar{R}_n| = \sqrt{\bar{C}_n^2 + \bar{S}_n^2}$ is the mean resultant of the n th trigonometric moment and $\bar{\theta}_n = \tan^{-1}(\frac{\bar{S}_n}{\bar{C}_n})$ is its direction. The first moment, $\bar{\theta}_1$, gives the mean angle of distribution of $p(\theta)$. $|\bar{R}_1|$ is the magnitude of the first trigonometric moment. It can take values between 0 and 1. If $|\bar{R}_1|$ is closer to 0, it means the multipath AOA are arriving at receiver over a wide range of angles. However, if AOA are restricted to small angular width about the mean position, θ_1 , then $|\bar{R}_1|$ will take larger value closer to 1. $|\bar{R}_1|$ is related to the shape factor angle spread, Λ , and standard deviation, σ_θ [13]:

$$\Lambda = \sqrt{1 - |\bar{R}_1|^2} \tag{7}$$

$$\sigma_\theta = \sqrt{-2 \ln(|\bar{R}_1|)} \tag{8}$$

where σ_θ is the standard deviation of the angular energy distribution in radians. The shape factors Λ and σ_θ are also inter-related as

$$\sigma_\theta = \sqrt{-\ln(1 - \Lambda^2)} \tag{9}$$

$$\Lambda = \sqrt{1 - e^{-\sigma_\theta^2}} \tag{10}$$

Angle spread is often measured in terms of the total span occupied by the non-zero values of occurrences [6]. It is denoted by θ_{span} and defined as

$$\theta_{\text{span}} = \theta_{\text{max}} - \theta_{\text{min}}$$

where θ_{max} and θ_{min} are maximum and minimum angles of arrival, respectively, of the PDF.

Moreover, two more shape factors i.e. the angular constriction, γ , and orientation parameter, θ_{MF} , have also been proposed in [13, 14]. γ also ranges between 0 and 1 and describes how multipath concentrates about two azimuthal directions with 1 indicating the concentration in two azimuth direction and 0 demonstrating no clear bias in two directions. θ_{MF} provides the azimuth direction of maximum fading. These two shape factors are defined as [13]

$$\gamma = \frac{|\overline{R}_2 - \overline{R}_1^2|}{1 - |\overline{R}_1|^2} \tag{11}$$

and

$$\theta_{\text{MF}} = \frac{1}{2} \text{phase}\{\overline{R}_2 - \overline{R}_1^2\} \tag{12}$$

Multipath shape factors are useful for studying fading statistics in non-omnidirectional multipath propagation channel. Fading statistics like level crossing rate, N_r , average fade duration, $\overline{\tau}$, auto-covariance, $p(r, \theta)$, and coherence distance, D_c , expressed in terms of multipath shape factors are defined as [13, 14].

The level crossing rate, N_r , is the measure of rapidity of fading and can be defined as

$$N_r = \sqrt{2\pi} \Lambda f_D \rho \sqrt{1 + \gamma \cos(2(\theta - \theta_{\text{MF}}))} \exp(-\rho^2) \tag{13}$$

where $f_D = \frac{v}{\lambda}$, and λ is the wavelength of the radiation.

The average fade duration, $\overline{\tau}$, is the time that the signal spends below the threshold level, ρ , and can be formulated as

$$\overline{\tau} = \frac{(\exp(-\rho^2) - 1)}{\sqrt{2\pi} f_D \Lambda \rho \sqrt{1 + \gamma \cos(2(\theta - \theta_{\text{MF}}))}} \tag{14}$$

The auto-covariance, $p(r, \theta)$, is envelope correlation between two points in space separated by a distance r in an azimuth direction θ . $p(r, \theta)$ can be defined as

$$p(r, \theta) = \exp\left[-23\Lambda^2(1 + \gamma[\cos 2(\theta - \theta_{\text{MF}})])\left(\frac{r}{\lambda}\right)^2\right] \tag{15}$$

The coherence distance, D_c , is the distance in space over which the channel response remains constant. D_c can be formulated as

$$D_c = \frac{\lambda \sqrt{\ln 2}}{\Lambda \sqrt{23(1 + \gamma[\cos 2(\theta - \theta_{MF})])}} \tag{16}$$

3 Results and discussion

The mathematical findings discussed in the previous section empower us to analyze the chosen spatial channel models and measurement data on the basis of second order statistics. Tables 1 and 2 enlist the first and second order statistics of the spatial channel measurements and models, respectively. Tables 1 and 2 show the numerical results obtained from simulating Eq. (1) to (12). From Table 1, it can be easily observed that θ_{span} has greater values for observation at MSs as compared to BSs for macrocellular models and measurements. It is in accordance to the fact that in macrocellular environment, scatterers are usually present in the vicinity of the MSs which

Table 1 Numerical values of second order statistics for spatial channel models and measurements in macrocellular environment

Environment	Macrocell		θ_{span}	$\bar{\theta}$ Mean	θ_{MF}	σ_θ S.D	Λ A.S	γ A.C
Measurements	Pedersen [7]	BS	50°	0.1°	-89.9°	7.08°	0.12	0.97
	Jalden [10]	BS	32°	8.41°	-78.8°	4.8°	0.08	0.99
	Jalden [10]	MS	100°	70.6°	-26.3°	19.2°	0.32	0.91
Models	CSM [2]	BS	17.2°	0.09	-89.8°	4.28°	0.07	0.99
	CSM [2]	MS	360°	0.5	0.5°	92.5°	0.96	0.67
	GSDM [5]	BS	50°	0	-90°	5.82°	0.10	0.99
	JGSM [6]	BS	50°	0	90°	6.33°	0.11	0.98
	JGSM [6]	MS	360°	0	0	119	0.99	0.10
	Nawaz [12]	MS	360°	-0.5	-0.5°	144°	0.99	0.64

Table 2 Numerical values of second order statistics for spatial channel models and measurements in picocellular environment

Environment	Picocell		θ_{span}	$\bar{\theta}$ Mean	θ_{MF}	σ_θ S.D	Λ A.S	γ A.C
Measurements	Cramer [9]	MS	360°	-2.6°	76.1°	38.6°	0.60	0.18
	Spencer [8]	MS	350°	11.7°	-77.2°	36.8°	0.58	0.18
	Zhang 1 [11]	MS	135°	-53.6°	72.7°	34.7°	0.55	0.80
	Zhang 2 [11]	MS	320°	10.2°	89.4°	34.1°	0.54	0.09
Models	ESM [2]	MS	360°	0	90°	51.6°	0.74	0.14
	Ecc-SM [6]	MS	100°	70.6°	-26.3°	19.2°	0.32	0.91

is in contrast to θ_{span} values at BSs which are usually free from scattering objects. That is why θ_{span} for the observations at MSs is greater than that for BSs. Moreover, in macrocellular environment, BSs are located at larger heights and separated from MSs over large distances. Due to this reason, multipath signals arrive at BS over small angular width which results in lower θ_{span} values at BS. However, θ_{span} has always higher values if AOAs are recorded at MS. From Table 1, it is observed that CSM at BS [2] shows the lowest θ_{span} . This is due the fact that CSM models the rural macrocellular environment where BSs are located at larger heights. Moreover, directional antenna employed in [3] also results in lower θ_{span} values at BS. On the other hand, GSDM [5] and JGSM [6] model the urban macrocellular environment where BSs are located at comparatively lower heights, so the high rise buildings near the BSs also cause scattering of multipath signals, which results in relatively greater θ_{span} for these spatial models. Similarly, Pedersen et al. [7] had a measurement campaign taken in urban macrocellular environment and its θ_{span} matches exactly to that of GSDM and JGSM. Jalden et al. [10] also had its measurement campaign in an urban environment but its θ_{span} is lower than the measurement campaign of Pedersen et al. [7], due to the reason that Jalden et al. employed directional antennas at BS and MS. θ_{span} values at MSs displayed by the spatial channel models are higher than those at BSs due to its lower location and dense scattering region supposed around MSs. However, the measurement campaign of Jalden et al. [10] at MS show lower θ_{span} due to the use of directional antenna as discussed for θ_{span} at BS. Table 1, also displays the values of standard deviation, σ_{θ} , for spatial channel models and measurements in macrocellular environment. The value of SD, σ_{θ} , for JGSM and GSDM has a close match to the measurement campaign of Pedersen et al. [7]. CSM at BS [3] shows the lowest SD, σ_{θ} , due to directional antennas equipped at BS. The values of SD, σ_{θ} , are higher for CSM at MS [3], and 3-D macrocellular model proposed by Nawaz et al. [12]. This is due to the fact that these pdfs are evaluated with directional antennas placed at BSs. However, the measurements of Jalden et al. [10] show lower values of SD, σ_{θ} , with directional antennas placed at BS and MS. The value of SD, σ_{θ} , are used for determining antenna spacing between antenna elements. Higher values of SD, σ_{θ} , for MS means that if directional antennas are employed at BS and MS then the operating at MS have to produce wider beam-width in comparison to those used at BS. Table 1, reveals the values of shape factor, Λ , for measurements and models in macrocellular environment. The values of shape factor, Λ , at BS for spatial measurements and models fall in the range of lower values i.e. 0–0.12. However, at MS the values of Λ fall in the range of higher values i.e. 0.32–0.99. This is due to the fact that the density of scatterers is higher in the vicinity of MS in macrocellular environment which results in increased value of Λ . However, BS are almost free from scatterers in rural macrocellular environment which results in lower values of Λ . The values of Λ for the spatial channel models proposed for urban macrocell like GSDM and JGSM match closely to the measurement campaign of Pedersen et al. [7], taken in urban environment. The value of shape factor angular constriction, γ , displayed in Table 1 are almost high at BS and MS in macrocellular environment. From these results, we can conclude that in macrocellular environment the multipath power is not distributed uniformly as is usually assumed, instead it arrives in cluster shape from several isolated directions. Table 2 displays the first and second order

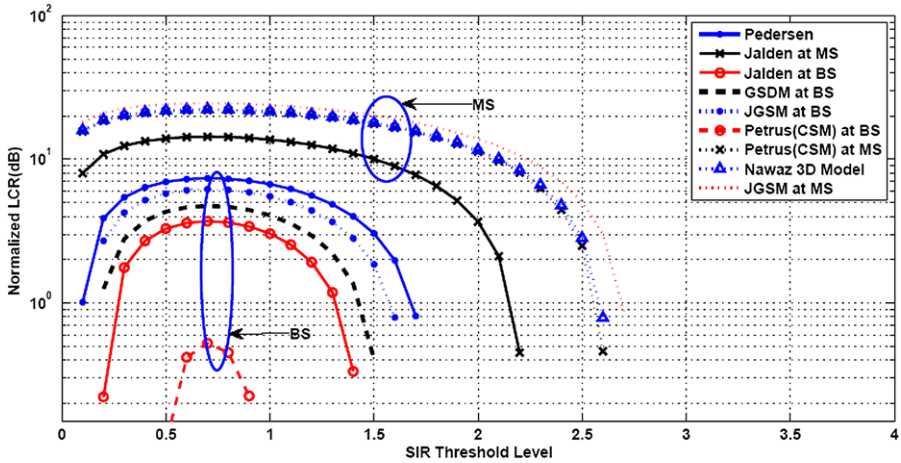


Fig. 1 Comparison of LCR of spatial channel models and measurements in macrocell

statistics of spatial channel models and measurements in picocellular environment. In picocellular environment, BSs and MSs are located at lower heights so the density of scatterers surrounding BSs and MSs is almost equal which results in almost equal θ_{span} values observed at BSs and MSs. From Table 2, it is observed that θ_{span} values for spatial channel models and measurements are higher at MS. However, the θ_{span} value for the measurement data of Zhang et al. [11] is smaller than the rest of the measurement campaigns. This is due the fact that these measurements are taken with directional antennas employed at MS. Table 2, also reveals higher values of SD, σ_{θ} , for spatial channel models and measurements. From these results we can say that MSs get multipath power over a wide range of angles both in pico- and macrocellular environment. The values of shape factor, Λ , falls in the range of higher values i.e. 0.54–0.94. This is due to the reason that in picocell the density of scatterers (doors, walls, shelves, windows, etc.) is higher which results in increased values of Λ at MS and BS. The values of shape factor, γ , is almost lower for the spatial channel models and measurements. From this we can conclude that in picocellular environment the multipath power is relatively more uniformly distributed in comparison to macrocellular environment.

Figures 1 and 2 show the plots of normalized level crossing rate i.e. versus increasing threshold level for spatial channel models and measurements in macro and picocellular environment, respectively. LCR are sensitive to the density of scatterers surrounding BS and MS. In Fig. 1, CSM at BS [3] shows the lowest LCR. This is due to the reason that CSM models a rural macrocellular environment where density of scatterers at BS is lower. Moreover in CSM, BSs are equipped with directional antennas which reduces the value of θ_{span} . As a result, the scatterers coming in the beam range of the directional antenna are also reduced which results in lower LCR curves at BS. LCR curves of GSDM and JGSM are higher comparatively due to the reason that these spatial models are used to model an urban macrocellular environment where density of scatterers at BS is higher in comparison to rural macrocell. The LCR curve of the measurement campaign of Pedersen et al. [7] has a close match to

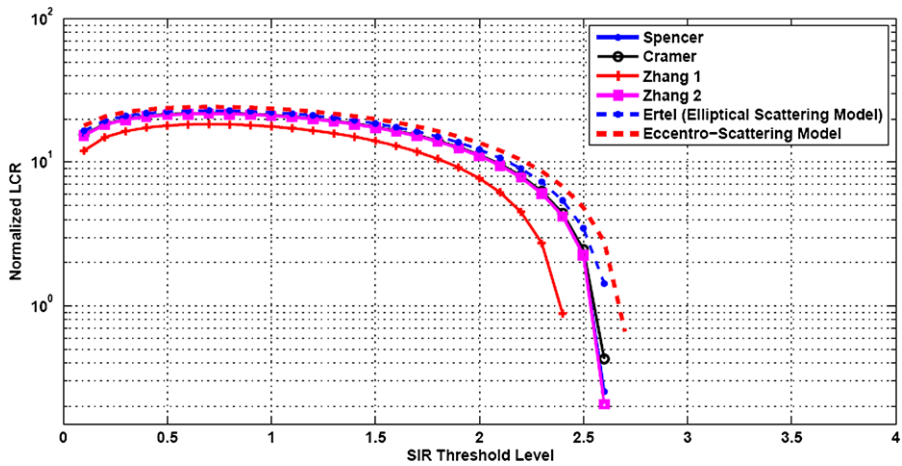


Fig. 2 Comparison of LCR of spatial channel models and measurements in picocell

that produced by JGSM. From this we can conclude that an urban macrocellular environment can be best modeled by JGSM. This conclusion can also be validated from the numerical results observed in Table 1. CSM at MS [2], JGSM at MS [6], Nawaz 3-D model at MS [12] show the highest LCR curves as shown in Fig. 1 due to dense scattering region around MS discussed earlier. The LCR curve of the measurement data of Jalden et al. at MS [10] shows a lower trend than the spatial channel models proposed at MS. Figure 2 shows the LCR curves of models and measurements in picocellular environment. LCR curves of the models and measurements in picocell show the same trend as shown by the spatial models and measurements in macrocell proposed at MS. From this we can conclude that the density of scatterers at MS remains the same independent of the physical propagation channel. Moreover, we can also say from the results displayed in Fig. 2 that the LCR curve of the measurement data of Ertel et al. [2] has a close match to the LCR curve of ESM proposed by Ertel et al. [2]. AFD curves of the spatial channel models and measurements displayed in Figs. 3 and 4, show the converse behavior as of LCR and thus can be explained and compared on the same basis as discussed above. CSM at BS [2], and Jalden et al. at BS [10], with the lowest θ span show the highest AFD while spatial channel models and measurements at MS with greater θ span show lowest AFD.

Figures 5 and 6 show the autocorrelation behavior of the spatial measurements and models plotted versus r/λ for macro and picocellular environment. High correlation behavior shows that the AOA distribution of that particular measurement is narrower. Figure 5 reveals that spatial channel models and measurements at BS show high correlation. These results can be validated from the numerical results listed in Table 1, where low values of SD, σ_θ , and angle spread, Λ , confirm such behavior for outdoor environment. This means that in macrocellular environment the multipath components arrive at the BS receiver array over small angular area which results in high correlation while in indoor environment the multipath components arrive at broadside to receiver array, which results in low correlations for indoor measure-

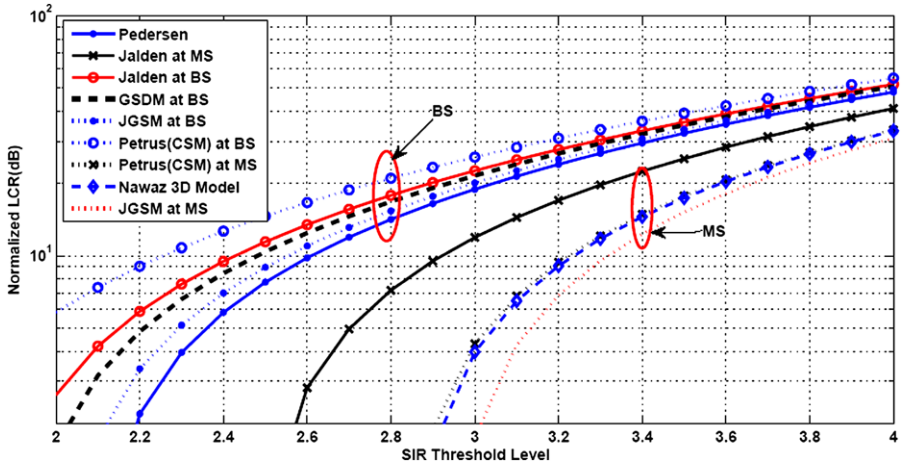


Fig. 3 Comparison of AFD of spatial channel models and measurements in macrocell

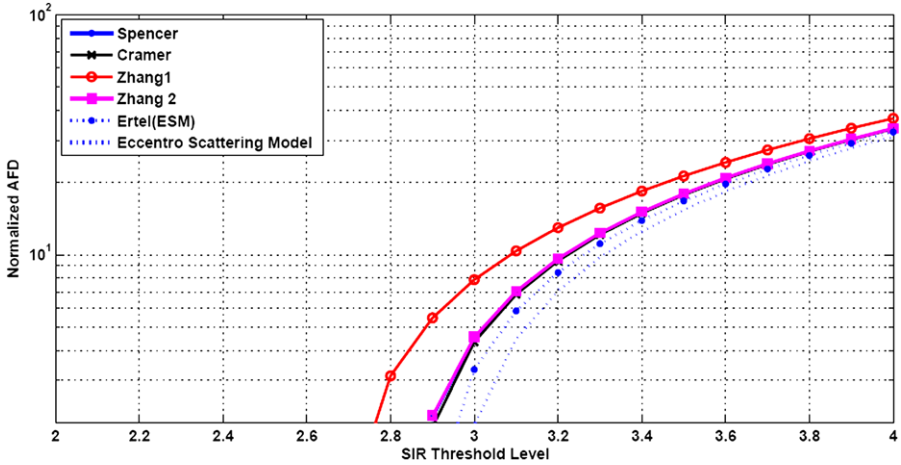


Fig. 4 Comparison of AFD of spatial channel models and measurements in picocell

ments. Results displayed in Fig. 5 show that the spatial channel models proposed at BS like CSM [2], GSDM [5], and JGSM [6], and spatial channel measurements like Pedersen et al. [7], Jalden et al. [10] show high correlations due to their low value of θ_{span} while correlations are low for the models and measurements proposed at MS in macrocellular environment. Figure 6 shows the correlations results displayed for picocellular environment. These correlations results follow the same trend as shown in Fig. 5 for correlations at MS. Figures 7 and 8 show the plots of coherence distance, D_c , versus λ . Coherence distance tells the degree of stability of a channel. Durgin et al. [13] proposed that as shape factor, Δ , increases, coherence distance decreases. According to the results shown in Fig. 7, CSM at BS [3] shows high coherence distance. The same spatial channel model shows the lowest shape factor, Δ , or SD, σ_θ , in

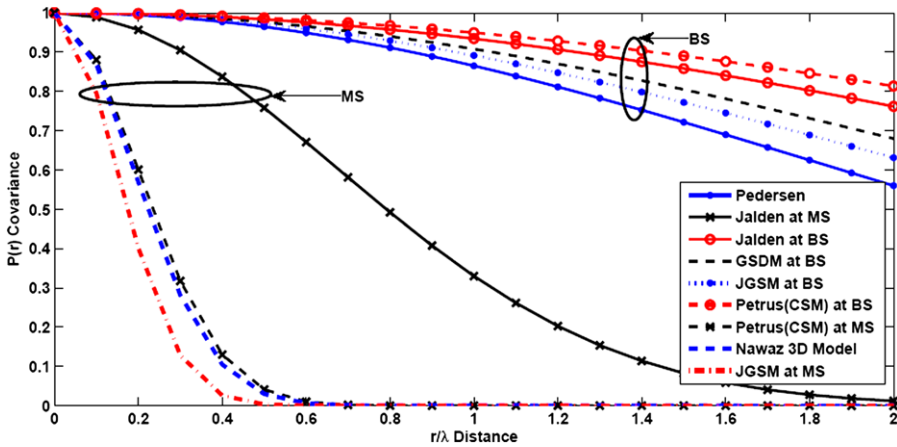


Fig. 5 Comparison of auto-covariance for spatial channel models and measurements in macrocell

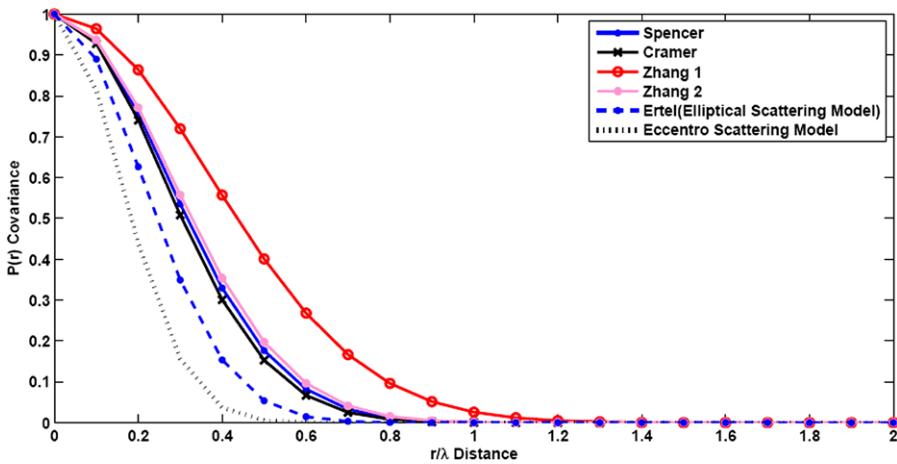


Fig. 6 Comparison of auto-covariance for spatial channel models and measurements in picocell

Table 1. In Fig. 3 we have already discussed that pdfs at BS show higher AFD curves. Large value of AFD and coherence distance show warnings about the instability of a cellular mobile channel. If a BS receiver goes in fade than due to the stability of the channel in the vicinity of the BS in macrocell (i.e. having no scatterers), will take longer time to come out of the fade.

Figures 9 and 10 show the plot of LCR versus different values of maximum Doppler frequency. LCR increases smoothly with Doppler frequency. These results follow the same trend as shown in [3]. LCR at MS is higher than that at BS. This is due to the dense scattered environment discussed earlier in the vicinity of MS which makes MS more sensitive to Doppler spread than BS. In Figs. 11 and 12, AFD reduces with increasing Doppler spread due to reciprocal behavior of AFD and LCR. The statistics of LCR and AFD are helpful in designing error control codes and diver-

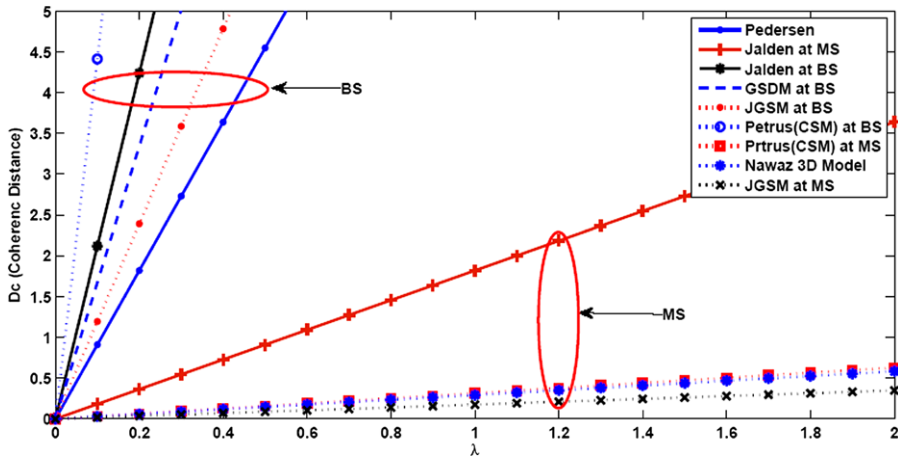


Fig. 7 Comparison of coherence distance for spatial channel models and measurements in macrocell

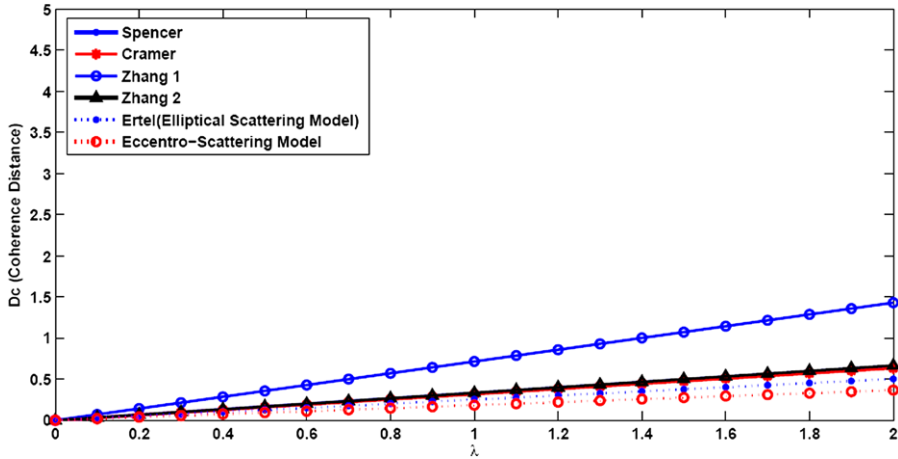


Fig. 8 Comparison of coherence distance for spatial channel models and measurements in picocell

sity schemes used in modern digital mobile communication system [15]. The SNR of the received signal is dependent on the velocity of moving MS. From Eq. (13), it can be observed that LCR has a direct relationship with the maximum Doppler frequency. Moreover, this direct dependence of LCR and the maximum Doppler frequency can be used to predict the maximum velocity of the MS for a given threshold level ρ [15]. When the velocity of the mobile increases, the Doppler frequency will also increase and shallow fades will be observed at MS with abrupt behavior of the received signal strength. Fade margin is an important characteristic of MS and BS transceiver system. If the fade margin of a transceiver goes below the particular threshold level, it will result in loss of bits. From Eq. (14), it is obvious that AFD has an inverse relationship with maximum Doppler frequency. If the maximum Doppler frequency is too low, while the signal are received with the power below the threshold, the transceiver will

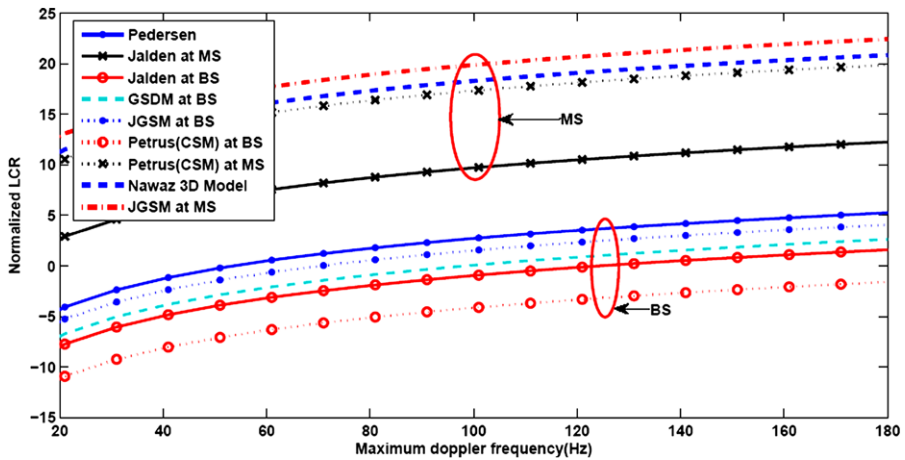


Fig. 9 LCR versus increasing Doppler spread for spatial channel models and measurements in macrocell

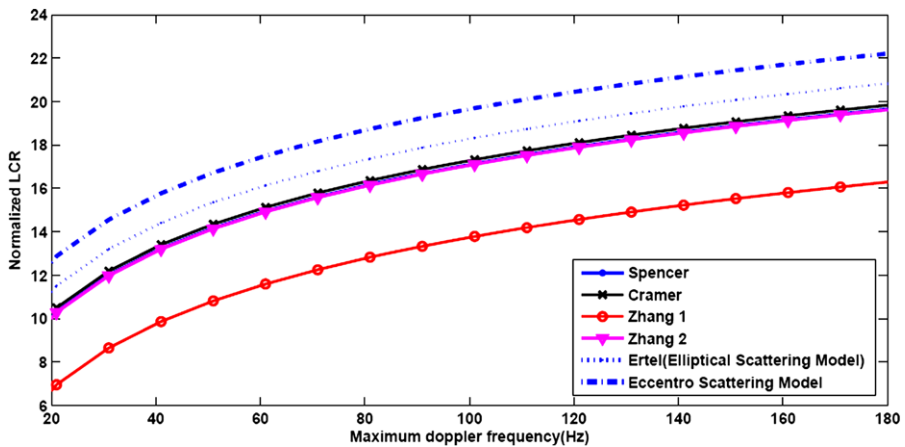


Fig. 10 LCR versus increasing Doppler spread for spatial channel models and measurements in picocell

remain in a deep fade for longer duration of time and most of the digital data will be lost during the fade. However, in case of the low Doppler spread, while the received power is above the threshold, the transceiver will continue receiving stronger signals for longer durations of time and the threshold level will not be crossed abruptly.

4 Conclusions

The fading statistics of the spatial channel models and measurements have been compared for goodness of fit, in order to validate the spatial channel models on the basis of their matching to the statistics of the measurements. Fading statistics have been evaluated using multipath shape factors considering macro and picocellular environments.

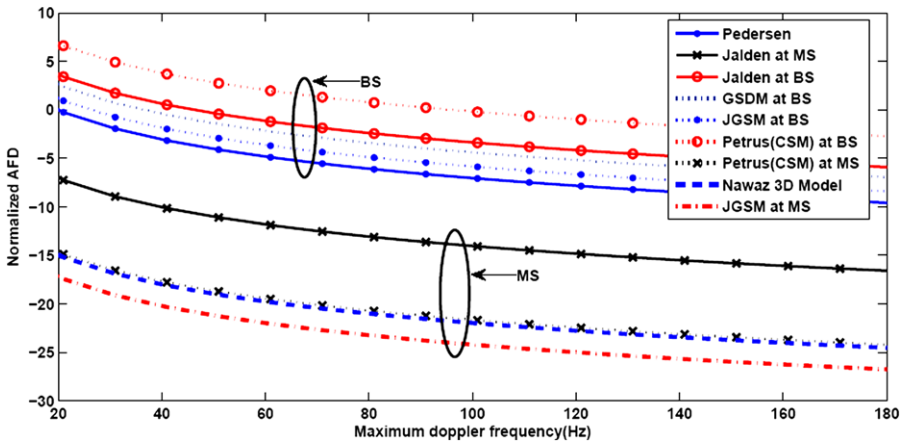


Fig. 11 AFD versus increasing Doppler spread for spatial channel models and measurements in macrocell

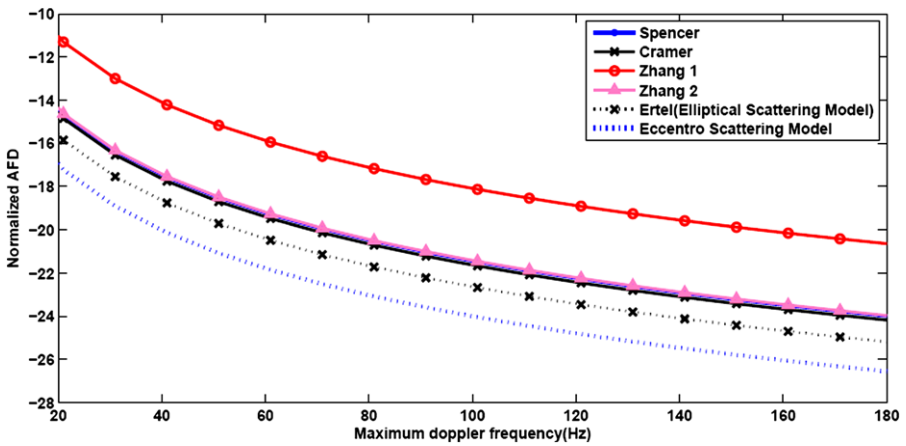


Fig. 12 AFD versus increasing Doppler spread for spatial channel models and measurements in picocell

Shape factors have been used which make it possible to analyze quantitatively some notable spatial channel models and field measurements having directional antennas at BS and MS. It has been observed that MSs surrounded by dense scattering region in macro or picocellular environments exhibit AOAs distributions over a wide angular span. In macrocellular environment, the multipath power is not distributed uniformly instead it arrives in cluster shape from several discrete directions. However, in picocellular environments the multipath power arrives more uniformly as compared to macrocellular environment. Fading statistics at MSs show the same behavior both in macro and picocellular environments. It has been revealed in results that MSs show high LCR than BSs. Directional antennas have a significant effect on the fading statistics. BS equipped with directional antennas show lower values of LCR. Therefore, it can also be predicted that directional antennas at MS may help reduce LCR at MS. Moreover, BSs have shown high correlations in macrocellular environment than MSs.

From this observation, we can conclude that BSs should preferably be equipped with beamforming systems. Moreover, MIMO systems are supposed to be committed to provide high data rates in future modern cellular communication systems like LTE-Advanced, and Broadband Wireless Man (WiMAX). A performance evaluation of a set of the separations among the array elements of these MIMO systems can be made more accurate and precise with the help of angle spread along with velocity dependent fading statistics discussed in this work. It has also been observed in results that the macrocellular environment can be best modeled by JGSM. On the other hand, in picocellular environment the fading statistics displayed by the ESM has a close match to the statistics of the indoor measurement data.

References

1. Jakes WC (1994) Microwave mobile communications. IEEE Press, Piscataway
2. Ertel RB, Reed JH (1999) Angle and time of arrival statistics for circular and elliptical scattering models. *IEEE J Sel Areas Commun* 17(11):1829–1840
3. Petrus P, Reed JH (2002) Geometrical-based statistical macrocell channel model for mobile environments. *IEEE Trans Commun* 50(3):495–502
4. Khan NM, Simsim MT, Rapajic PB (2008) A generalized model for the spatial characteristics of the cellular mobile channel. *IEEE Trans Veh Technol* 57(1):22
5. Janaswamy R (2002) Angle and time of arrival statistics for the Gaussian scatter density model. *IEEE Trans Wirel Commun* 1(3):488–497
6. Khan NM (2006) Modeling and characterization of multipath fading channels in cellular mobile communication system. PhD thesis dissertation, School of Electrical Engineering and Telecommunication, University of New South Wales (UNSW), Australia, March 2006
7. Pedersen KI, Mogensen PE, Fleury BH (2000) A stochastic model of the temporal and azimuthal dispersion seen at the base station in outdoor propagation environment. *IEEE Trans Veh Technol* 49(2):437–447
8. Spencer QH, Jeffs BD, Jensen MA, Swindlehurst AL (2000) Modeling the statistical time and angle of arrival characteristics of an indoor multipath channel. *IEEE J Sel Areas Commun* 18(3):347–360
9. Cramer RJ-M, Win MZ, Scholtz RA (1998) Impulse radio multipath characteristics and diversity reception. *IEEE Conf Commun* 3:1650–1654
10. Jalden N, Zetterberg P, Ottersten B, Garcia L (2007) Inter- and intrasite correlations of large-scale parameters from microcellular measurements at 1800 MHz. *EURASIP J Wirel Commun Netw*
11. Zhang Y, Brown AK, Malik WQ, Edwardes DJ (2008) High resolution 3-D angle of arrival determination for indoor UWB multipath propagation. *IEEE Trans Wirel Commun* 7(8):3047–3055
12. Nawaz SJ, Qureshi BH, Khan NM (2010) A generalized 3-D scattering model for macrocell environment with directional antenna at BS. *IEEE Trans Veh Technol* 59(7):3193–3204
13. Durgin GD, Rappaport TS (2000) Theory of multipath shape factors for small-scale fading wireless channels. *IEEE Trans Antennas Propag* 48(5):682–693
14. Durgin GD, Rappaport TS (1998) Basic relationship between multipath angular spread and narrow band fading in wireless channels. *IEE Electron Lett* 24(25):2431–2432
15. Rappaport TS (2002) Wireless communications, principles and practice, 2nd edn. Prentice Hall, Upper Saddle River